THE UNIVERSITY OF ALABAMA AT BIRMINGHAM

Knowledge that will change your world

GBSC 724
March 20, 2023

Real-time connection of Metabolomics with Medicine and Surgery and the rest of life

Stephen Barnes, PhD, FASN
Professor of Pharmacology & Toxicology
Director, Targeted Metabolomics and Proteomics Laboratory

Targeted Metabolomics & Proteomics Laboratory

1

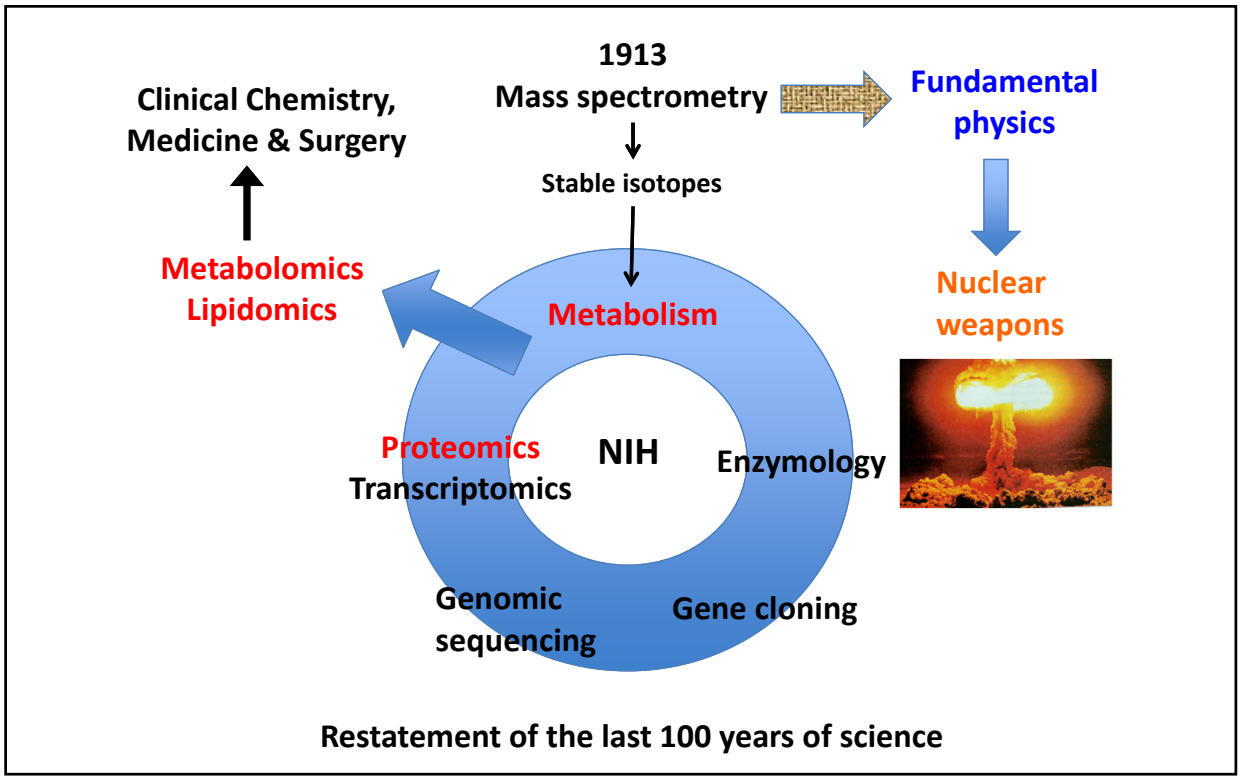

Restatement of the last 100 years of science

2

Dissociative research

- Samples are collected and stored for analysis at a "later" time
- "Later" can be months or years after sample collection
  - Of little direct benefit to the patient
  - Although may influence the community of patients
  - True of many analyses

3

Link to videos by James Kinross

Colorectal surgeon from Imperial College, London
Plenary Speaker at the UAB 2016 Metabolomics Workshop

http://www.uab.edu/proteomics/metabolomics/workshop/2016/videos/kinross_day2.html

http://www.uab.edu/proteomics/metabolomics/workshop/2016/videos/kinross2_day2.html

4

Real time analysis

- Existing, familiar applications
- Gases!
- The iknife
  - GI surgery
  - Cancer margins
  - Pathology
- DESI
- CARS
- Raman

5

Real-time analysis

- We see the real-time use of MS when we go through security checks at the airport
  - Checks for ion signatures of explosives

- Other devices are used to check for specific volatiles in the breath

6

Noses and smell – real time analysis

The superior volatile metabolite detector

7

Gases produced in the GI tract

- **H_2, CO_2 and CH_4 from carbohydrates**
  - ***Firmicutes***
  - **From pyruvate and NAD(P)H/$FADH_2$**
  - **H_2 used by sulfate-reducing bacteria (SRBs), methanogenic Archaea, and acetogens**
- **SRBs produce H_2S**
- **NO from nitrates**

8

Methods for measuring gases

Technology	Operation mode	Target intestinal gas	Detection limit	Cross-sensitivity	Response time	Life time	Estimated cost
Spectrometry based[a]							
GC-MS	Off line	All gases	ppt to ppb	Low	~Several minutes	Long	>US$300k
IMS	Real time	All gases	ppb	Low	<1 min	Long	>US$100k
PTR-MS	Real time	All gases	ppt	Low	<1 min	Long	>US$400k
SIFT-MS	Real time	All gases	ppb	Low	<1 min	Long	>US$400k
LS	Real time	Most gases except H_2	ppt to ppb	Low	<1 min	Long	<US$50k
Sensor based[b]							
Electrochemical	Real time	H_2, H_2S, NO, and CO_2	ppm	Medium	<30 s	Short	<US$100
Calorimetric	Real time	H_2, CH_4, and CO_2	ppt	High	<10 s	Medium	<US$100
NDIR	Real time	CO_2, CH_4, and VOCs	ppm to ppt	Low	<20 s	Long	<US$300

GC-MS gas chromatography-mass spectrometry
IMS ion mobility mass spectrometry
PTR-MS proton transfer reaction mass spectrometry
SIFT-MS selection ion flow tube-mass spectrometry
LS laser spectrometry

Jian Zhen Ou et al., Trends Biotech, 2015

9

Device for measuring fecal gas production

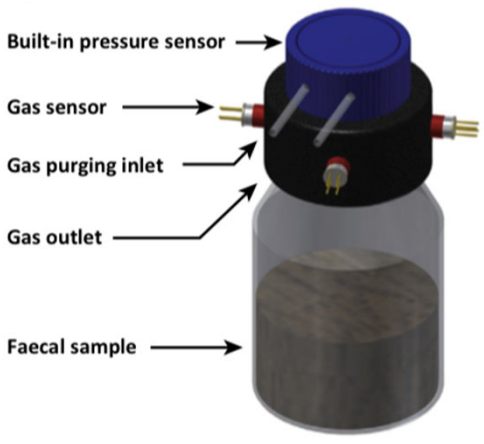

Jian Zhen Ou et al., Trends Biotech, 2015

10

Fecal gas production (ex vivo)

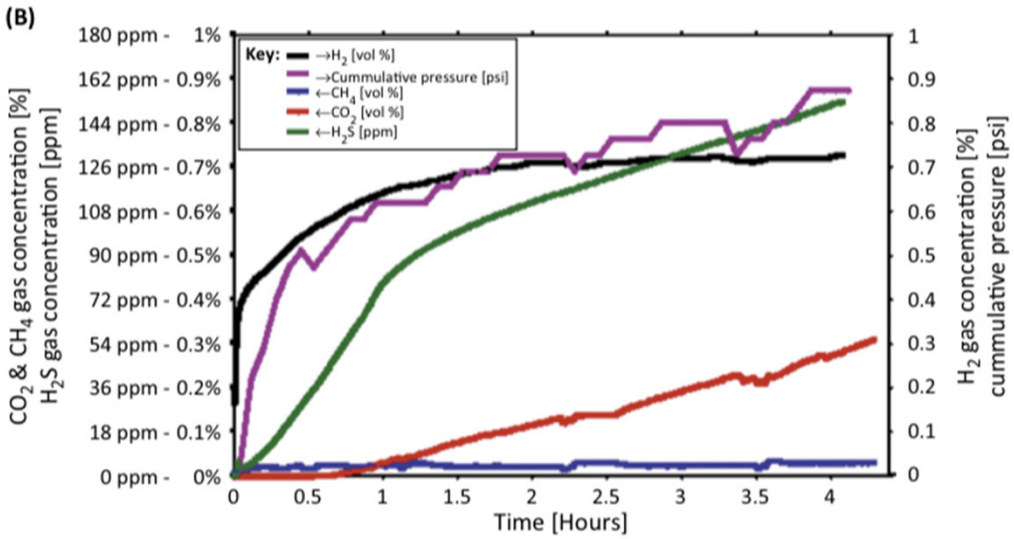

Jian Zhen Ou et al., Trends Biotech, 2015

11

Real-time *in situ* monitoring gas production

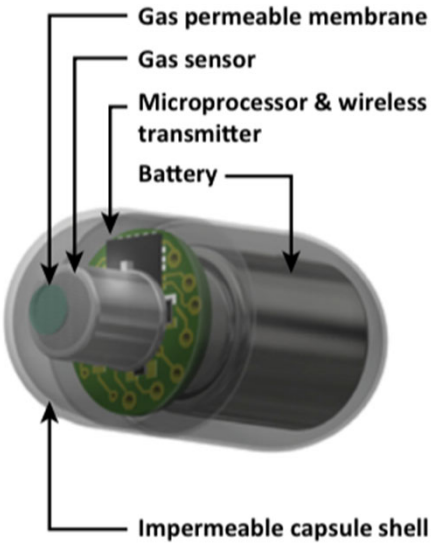

- The device is swallowed
- Completes full mouth-to-anus transit, reporting data as it goes
- Also provides positional information
- Operates at 405, 433, and 915 MHz
- Uses Lithium batteries!!

Jian Zhen Ou et al., Trends Biotech, 2015

12

Real time intestinal gas production

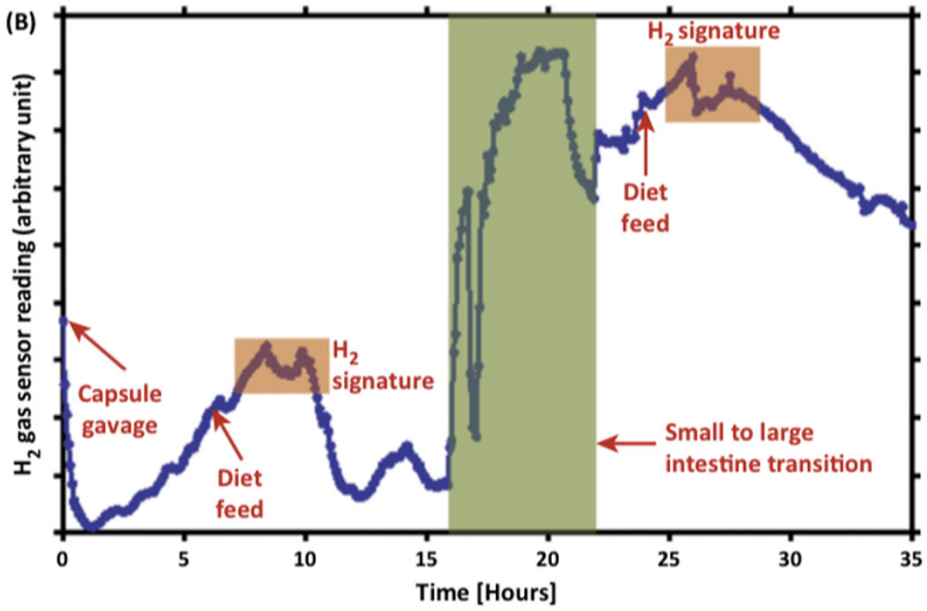

Jian Zhen Ou et al., Trends Biotech, 2015

13

The Challenge for Mass Spec

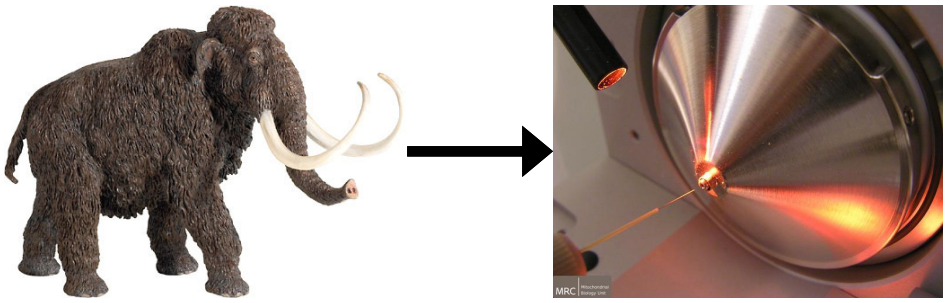

How to get the mammoth into the gas phase for analysis?

14

Droplet principle of electrospray

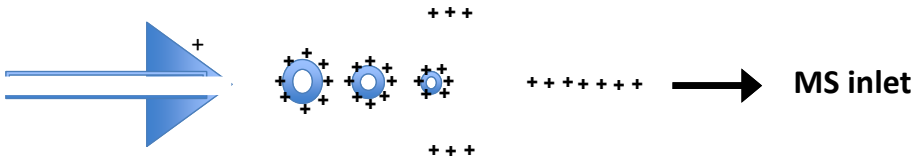

Droplet spray

- **Sneeze**
- **Lung motion**
- **Surgical knife**
- **Other vapors**

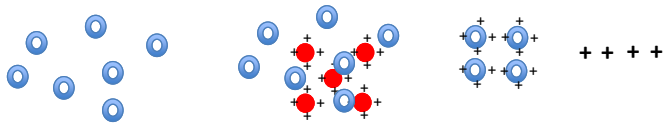

15

iKnife device

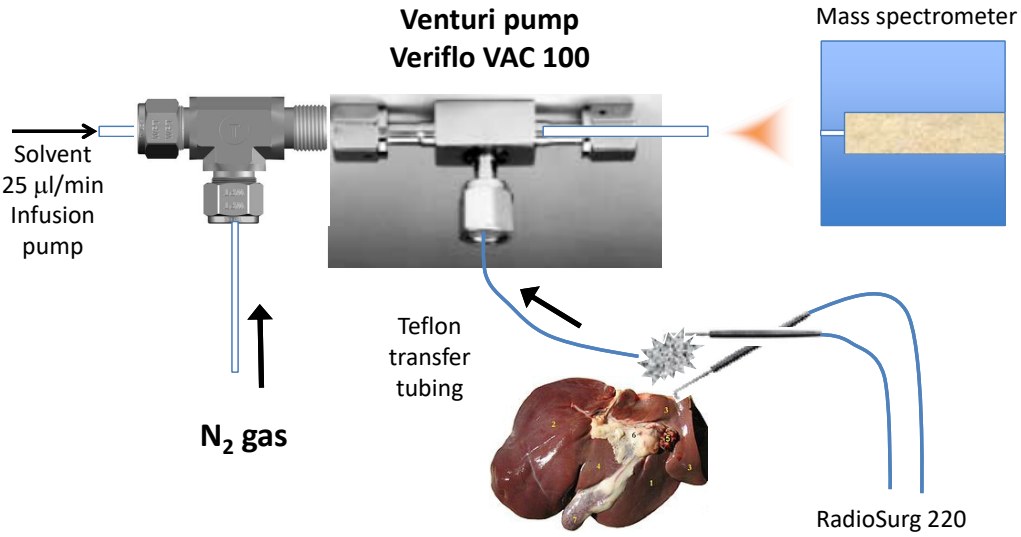

16

Mass spectrum of canine stomach

Predominantly phospholipids

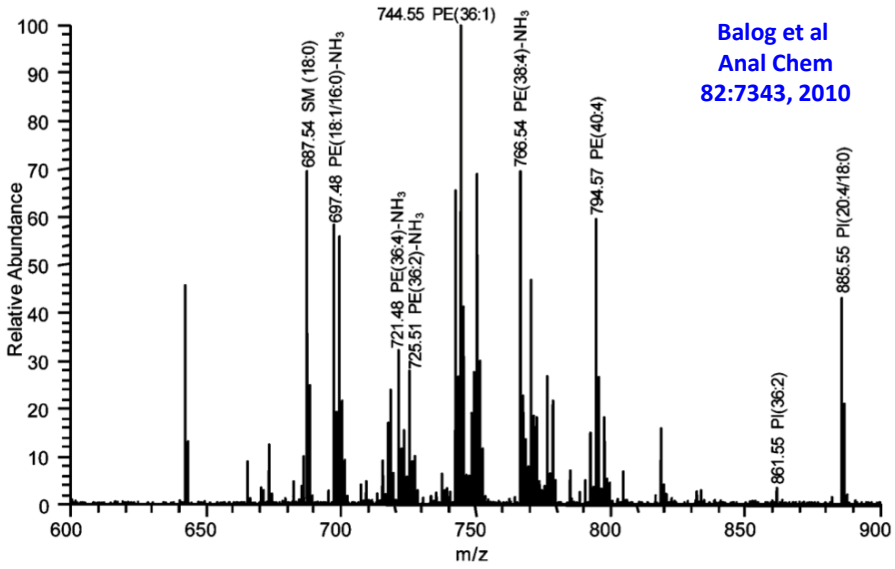

Balog et al
Anal Chem
82:7343, 2010

17

Phospholipid patterns are characteristic of cells and tissues

- Single items are not sufficient as biomarkers
- The classes of phospholipids and their fatty acid composition contain pattern discriminators
- In the absence of known classifiers, principal components analysis looks for groups of components that have the larger sources of variation
  - An individual sample's contributions to these groups are plotted in a 2D or 3D manner

18

Principal components analysis of ions from surgical "smoke"

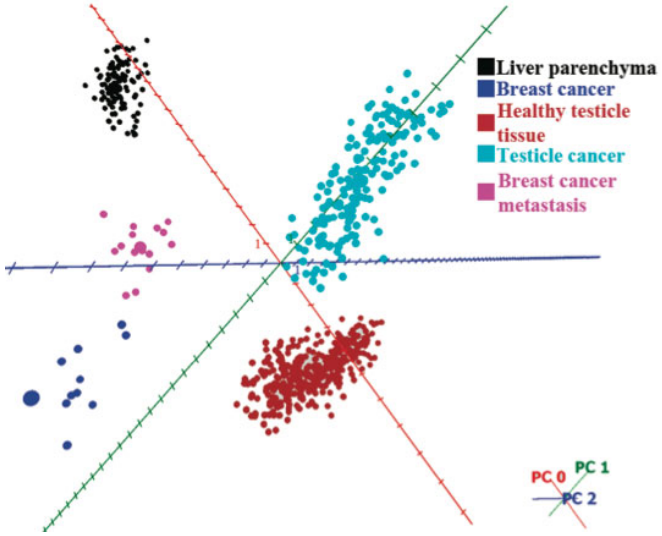

Balog et al
Anal Chem
82:7343, 2010

19

Differentiation of brain tumors

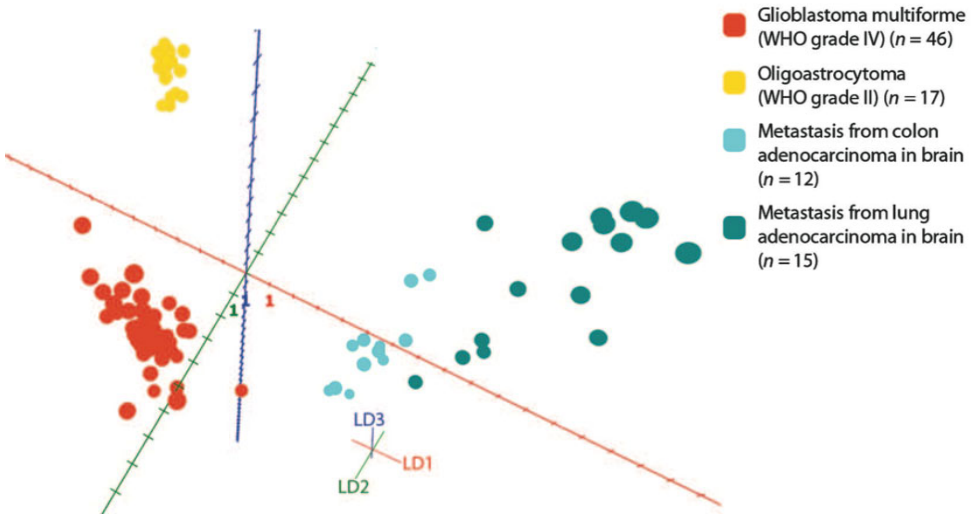

20

Changing lipids across cancer margin

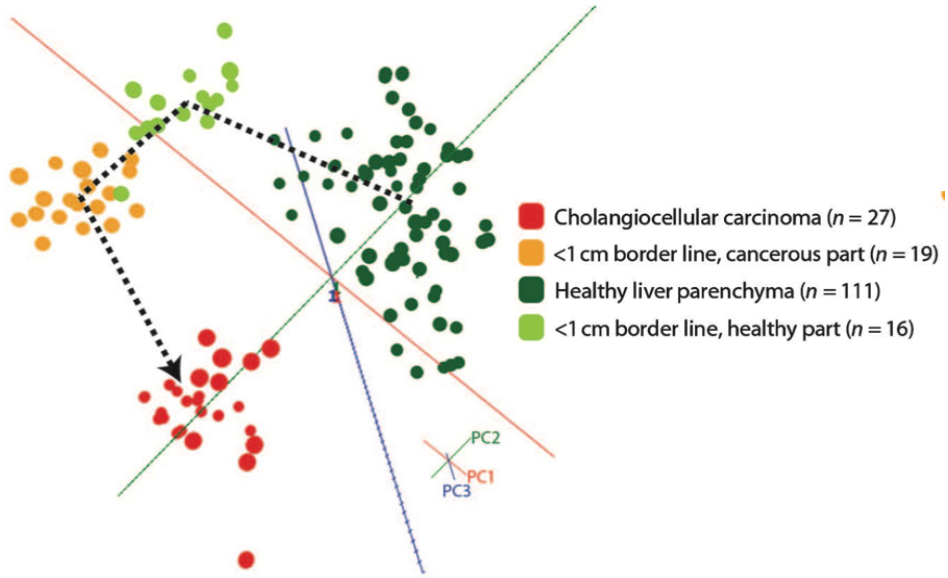

21

Adding real-time imaging – breast cancer

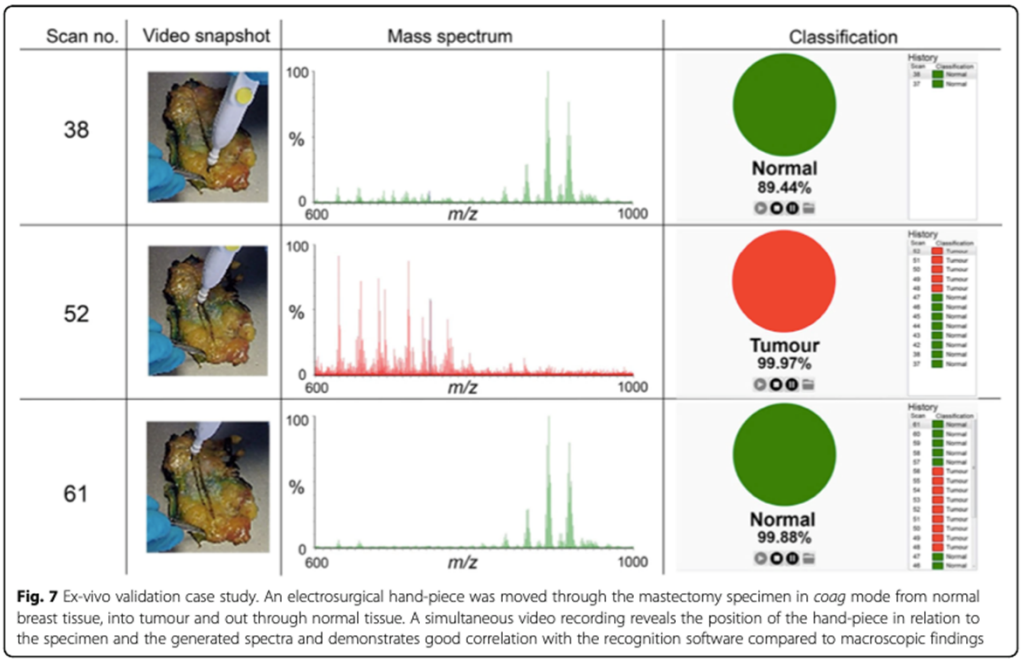

Fig. 7 Ex-vivo validation case study. An electrosurgical hand-piece was moved through the mastectomy specimen in *coag* mode from normal breast tissue, into tumour and out through normal tissue. A simultaneous video recording reveals the position of the hand-piece in relation to the specimen and the generated spectra and demonstrates good correlation with the recognition software compared to macroscopic findings

22

Computer-driven, Rapid Evaporative Imaging MS (REIMS) for tissue sections

23

Examining tissue (slices) by REIMS

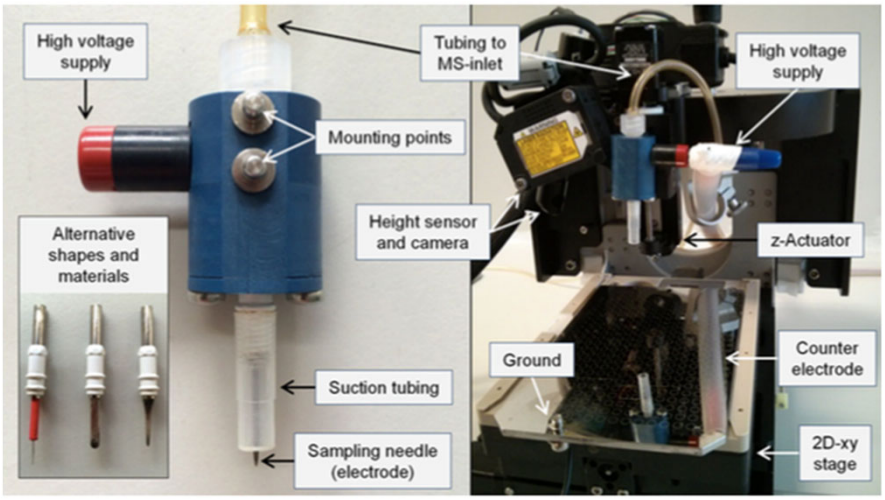

Golf et al., Anal Chem 2015

24

Modes of data acquisition for REIMS

Line Scans:
Cutting Mode

Individual Pixels:
Pointing Mode

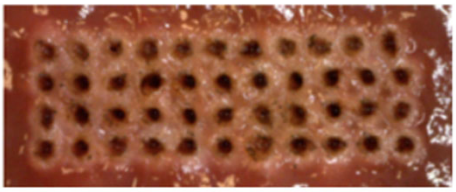

Golf et al., Anal Chem 2015

25

PCA analysis of REIMS data from tissue sections

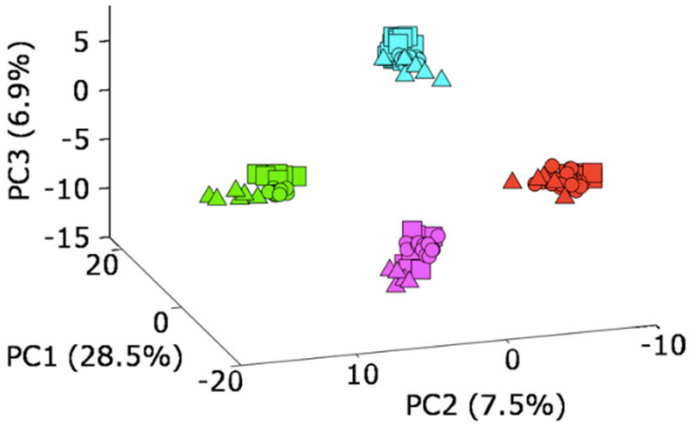

Golf et al., Anal Chem 2015

26

Application of iKnife to HPV and cancer

A

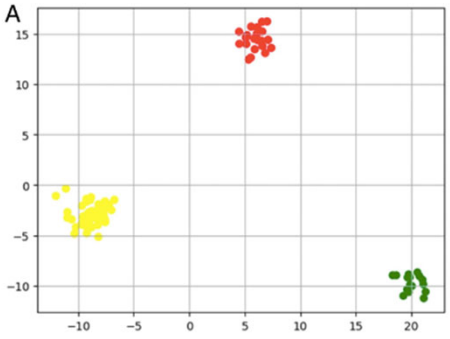

B

Proportion (%) of classification when correlating iKnife diagnosis to gold standard histology				
Predicted iKnife diagnosis	Histopathological Diagnosis			Cross Validation
	Normal (n=16)	HPV ± CIN (n=50)	Cancer (n=21)	
Normal	100% (16/16)	0% (0/50)	0% (0/21)	100%
HPV±CIN	0% (0/16)	100% (50/50)	0% (0/21)	
Cancer	0% (0/16)	0% (0/50)	100% (21/21)	

Normal Cervical Tissue
HPV ± CIN
Cancerous Cervical Tissue

Tzafetas M et al., PNAS, March 2020

27

Desorption electrospray ionization (DESI)

- Works by directing an electrical fine spray at a tissue target – does not require deposition of a matrix

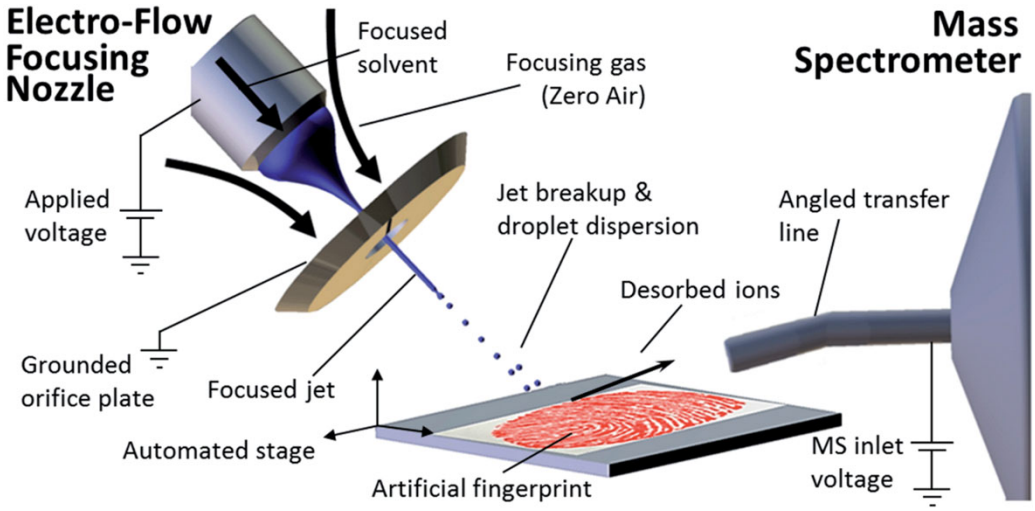

http://pubs.rsc.org/services/images/RSCpubs.ePlatform.Service.FreeContent.ImageService.svc/ImageService/Articleimage/2014/AN/c4an00172a/c4an00172a-f1_hi-res.gif

28

The IDH story of brain and other tumors

- IDH1 (isocitrate dehydrogenase) is mutated in position 132 in a GWAS study of patients with glioblastomas
- IDH1 catalyzes the conversion of isocitrate to alpha-ketoglutarate (αKG) which is a two-step reaction
- Mutant IDH1 catalyzes the first step – to 2-hydroxyglutarate (2HG), but not the second one to αKG
- 2HG is considered to be an onco-metabolite
- Note that it has two stereoisomers
- What follows is a study from a group at Harvard – performed in the Advanced Multimodality Image Guided Operating Suite at Brigham and Women's Hospital

29

Whither 2-hydroxyglutarate?

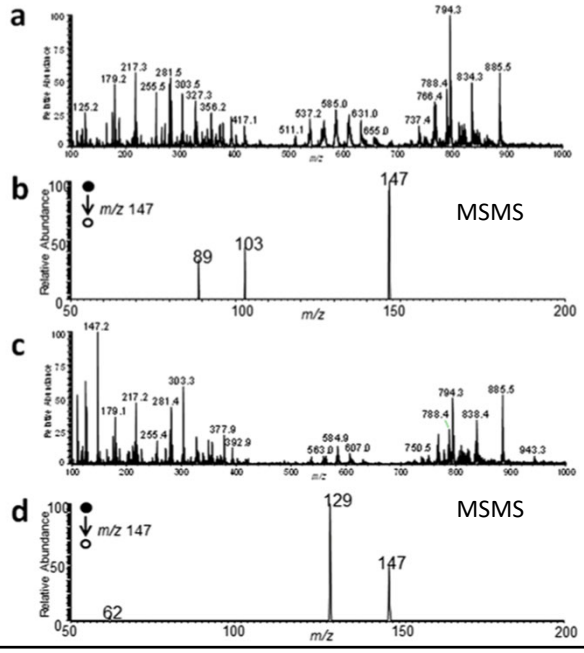

Tissue expressing wild type IDH1

MSMS of *m/z* 147 - not 2HG

Tissue expressing mutant IDH1

MSMS of *m/z* 147 is 2HG

Santagata et al. PNAS 2014

30

Value of exact mass – "147" vs "147"

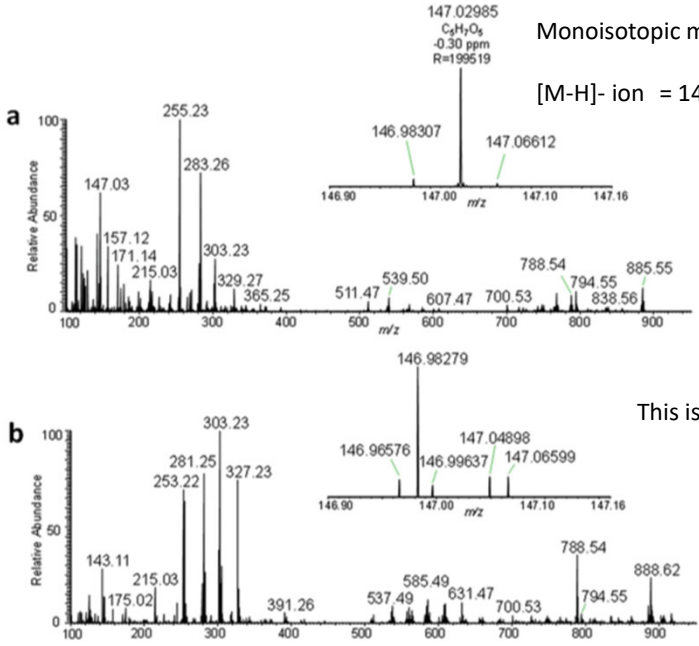

Monoisotopic mass of 2HG
= 148.037
[M-H]- ion = 148.037-1.00725
= 147.030

This is not 2HG

Santagata et al. PNAS 2014

31

Tumor xenograft imaging and 2HG

The ion at *m/z* 146.9 was subjected to MSMS to measure 2HG

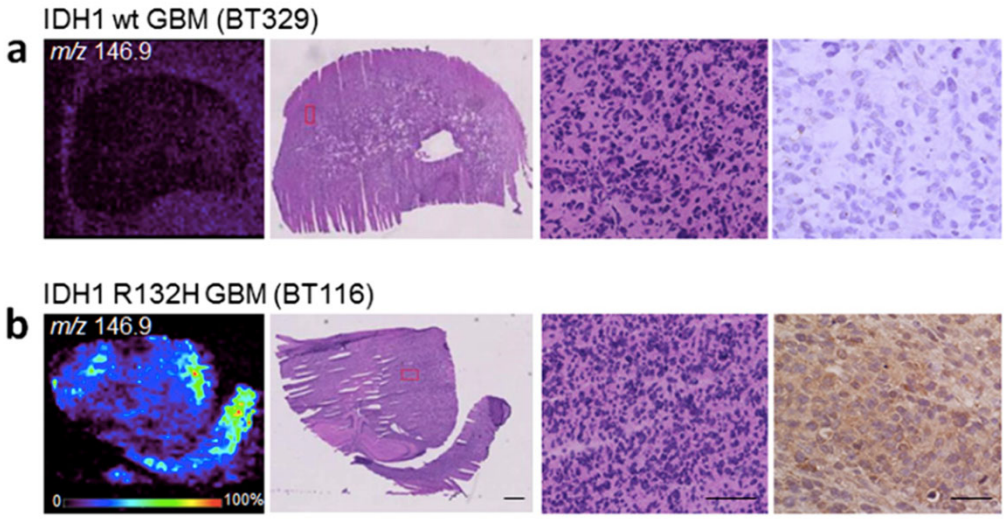

Santagata et al. PNAS 2014

32

Application to human glioblastoma

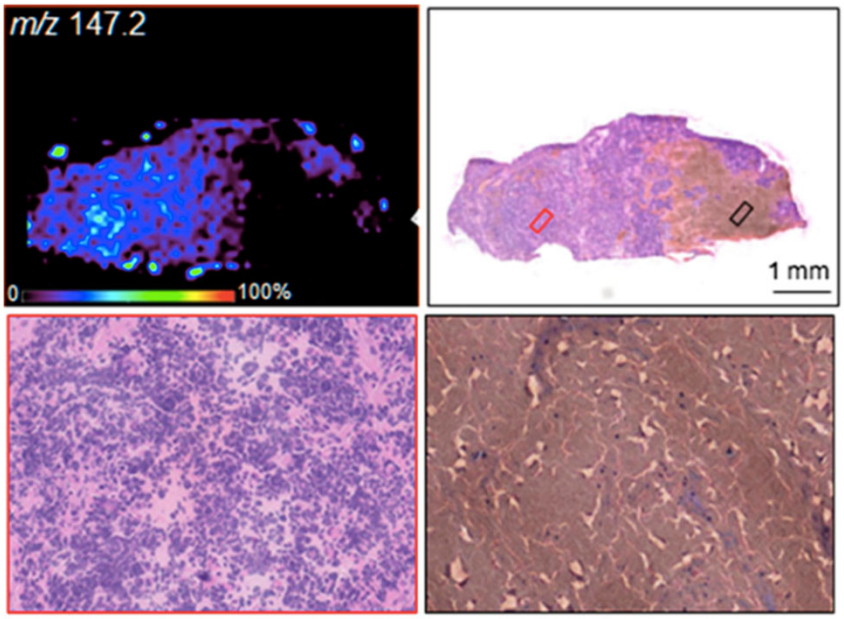

Santagata et al. PNAS 2014

33

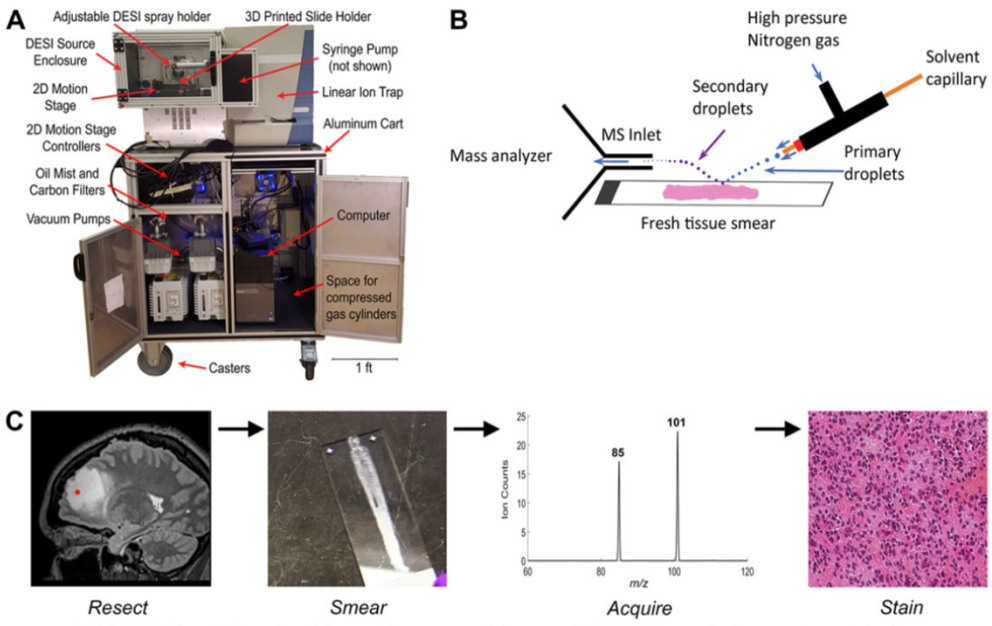

FIG. 1. DESI-MS method overview. **A:** Image of the custom-made intraoperative DESI-MS system for intraoperative analysis of tissue biopsies. **B:** Diagram of the DESI process as described by Takáts et al. **C:** Workflow of intraoperative analysis protocol consisting of tissue collection (*red spot*) and smearing, DESI-MS analysis, and post hoc histopathological staining. Original magnification ×20. Figure is available in color online only.

Alfaro et al., J Neurosurg (2019) Jan 4 1-8

34

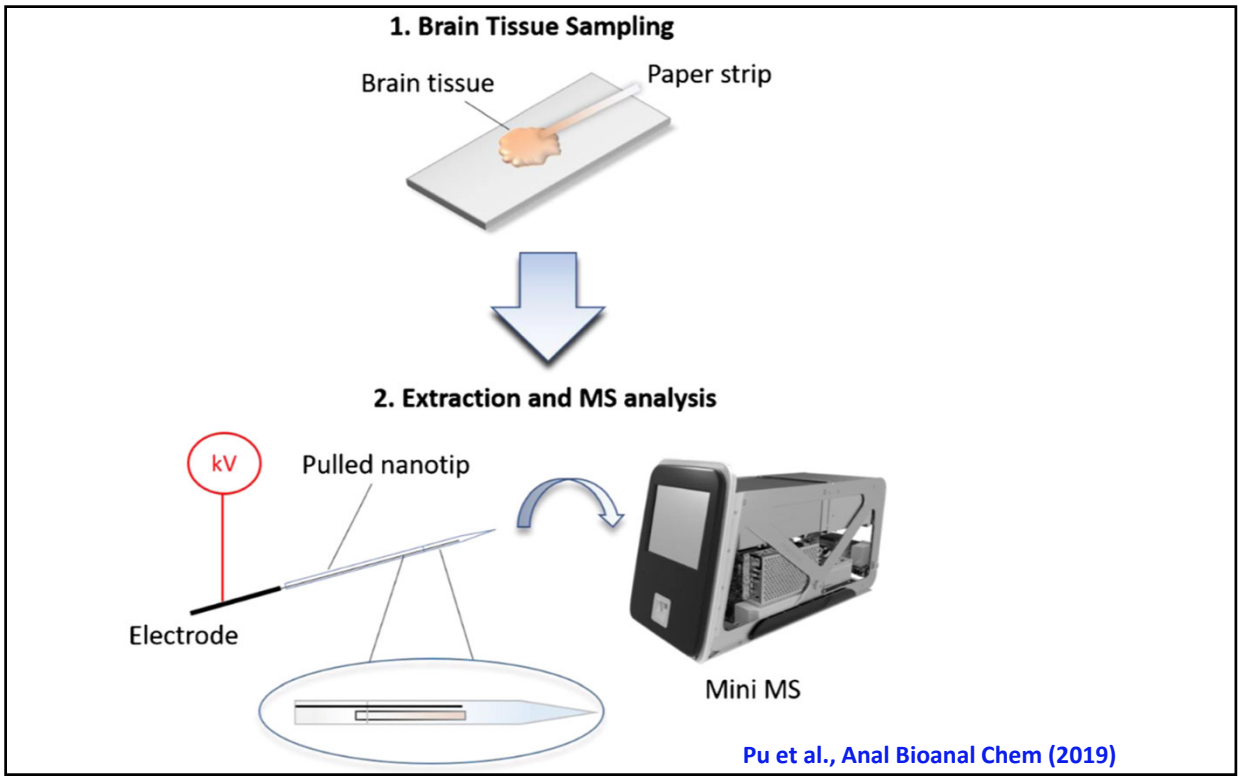

Pu et al., Anal Bioanal Chem (2019)

35

Comparative imaging of normal-tumor tissue transition

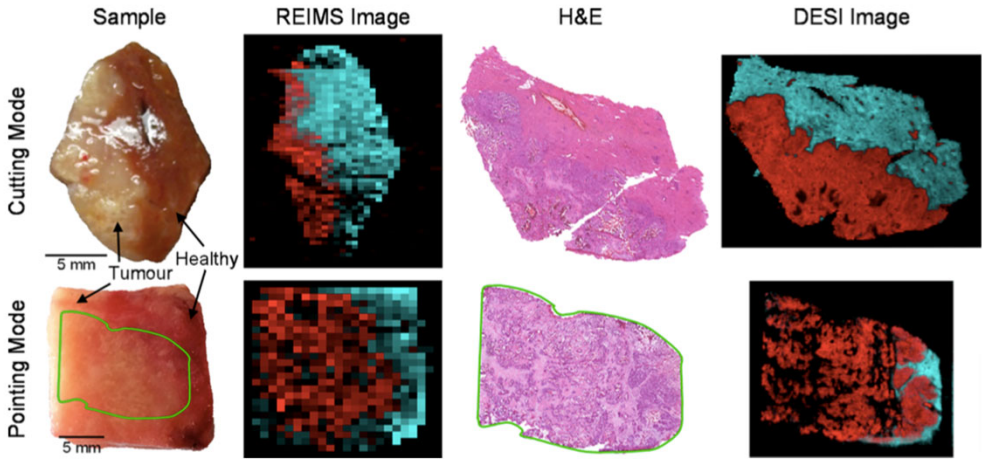

Golf et al., Anal Chem 2015

36

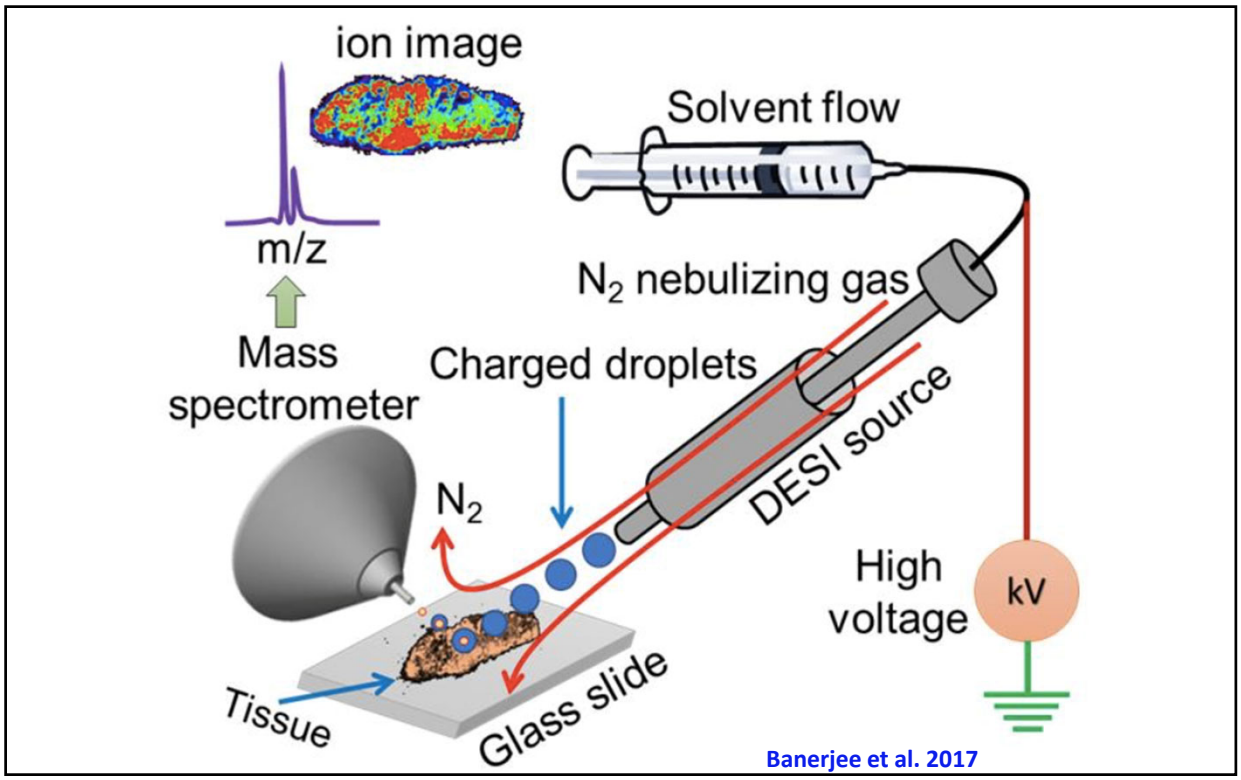

Banerjee et al. 2017

37

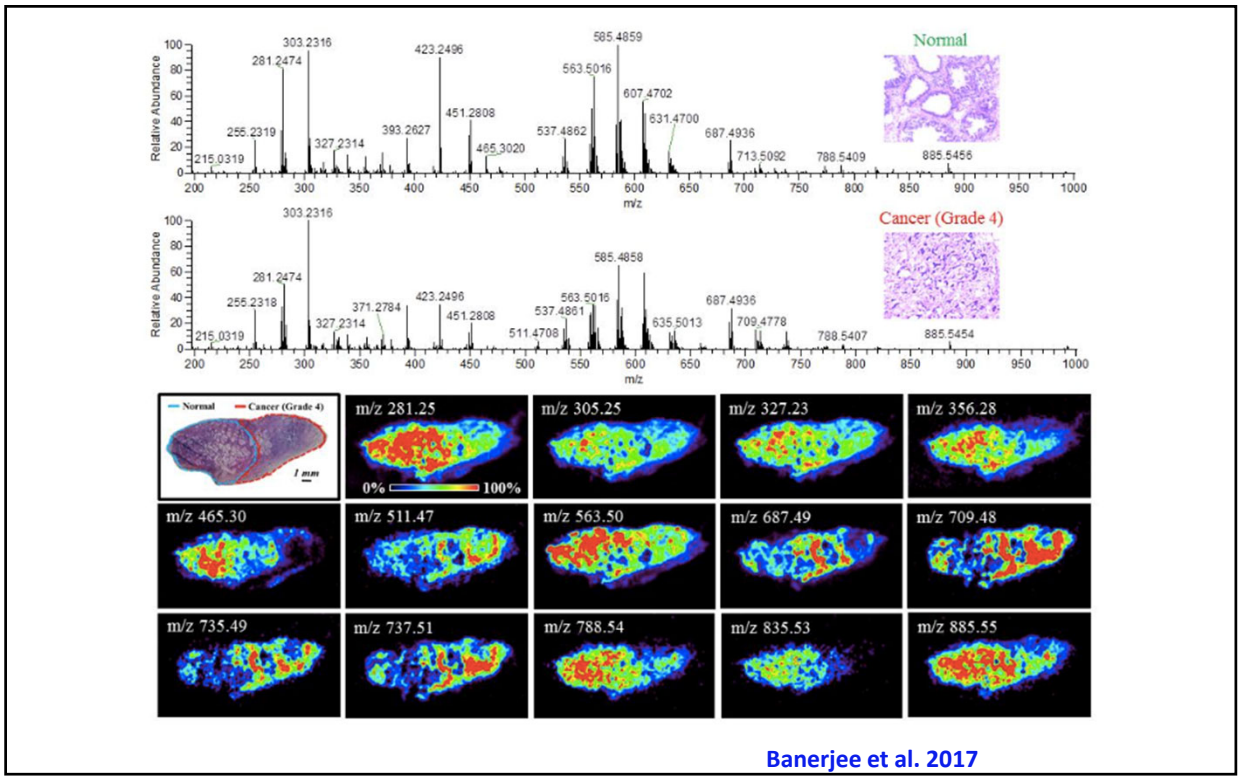

Banerjee et al. 2017

38

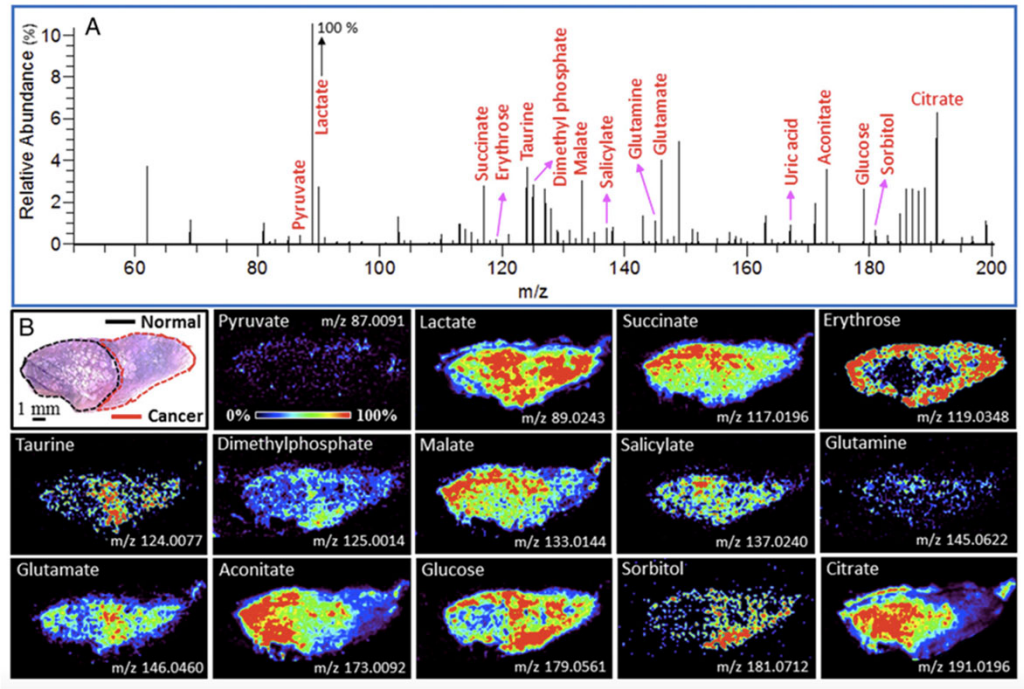

Banerjee et al. 2017

39

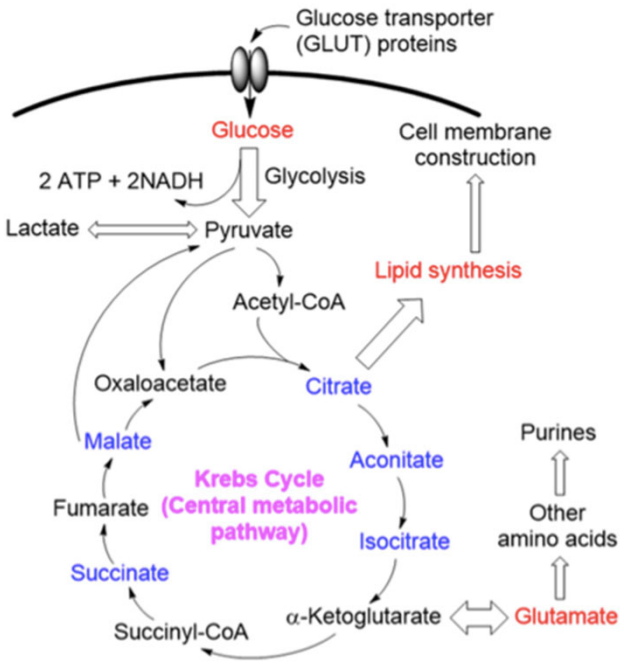

Red = elevated in cancer
Blue = down in cancer

40

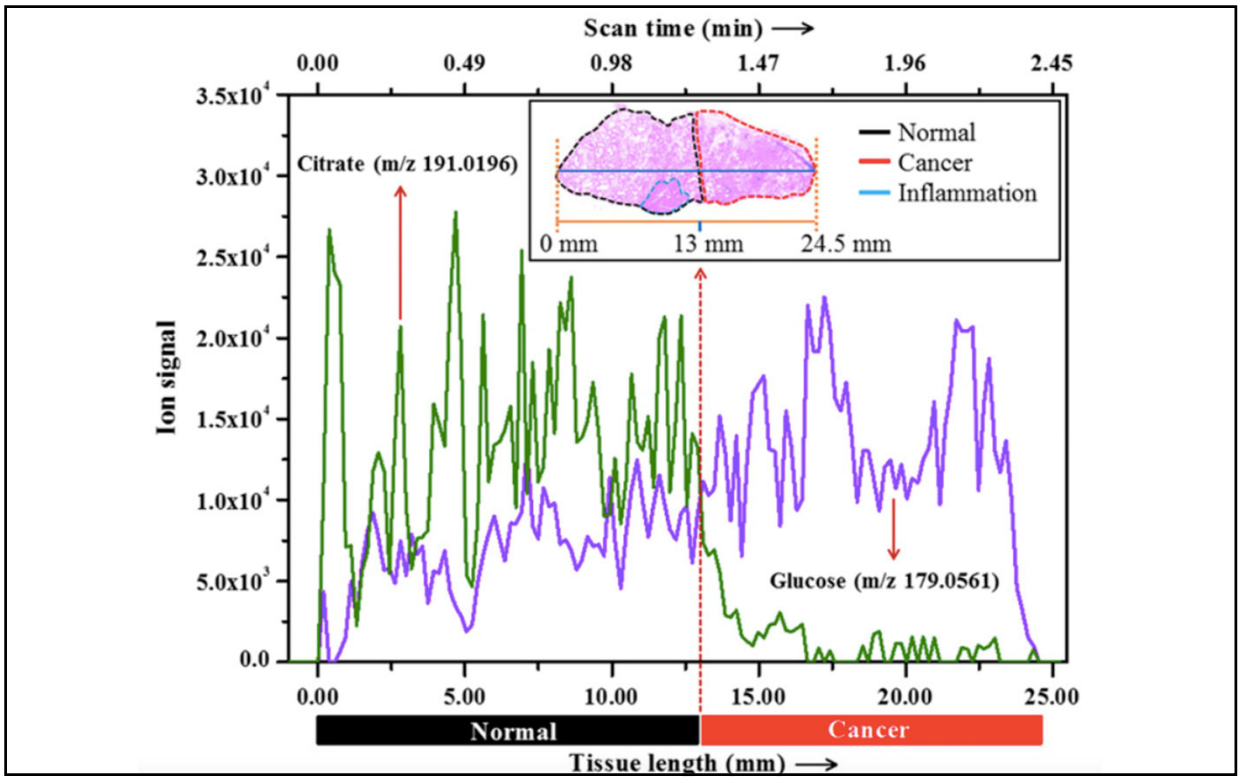
Scan time (min) ⟶
0.00
0.49
0.98
1.47
1.96
2.45
Ion signal
3.5x10⁴
3.0x10⁴
2.5x10⁴
2.0x10⁴
1.5x10⁴
1.0x10⁴
5.0x10³
0.0
Citrate (m/z 191.0196)
Normal
Cancer
Inflammation
0 mm
13 mm
24.5 mm
Glucose (m/z 179.0561)
0.00
5.00
10.00
15.00
20.00
25.00
Normal
Cancer
Tissue length (mm) ⟶

41

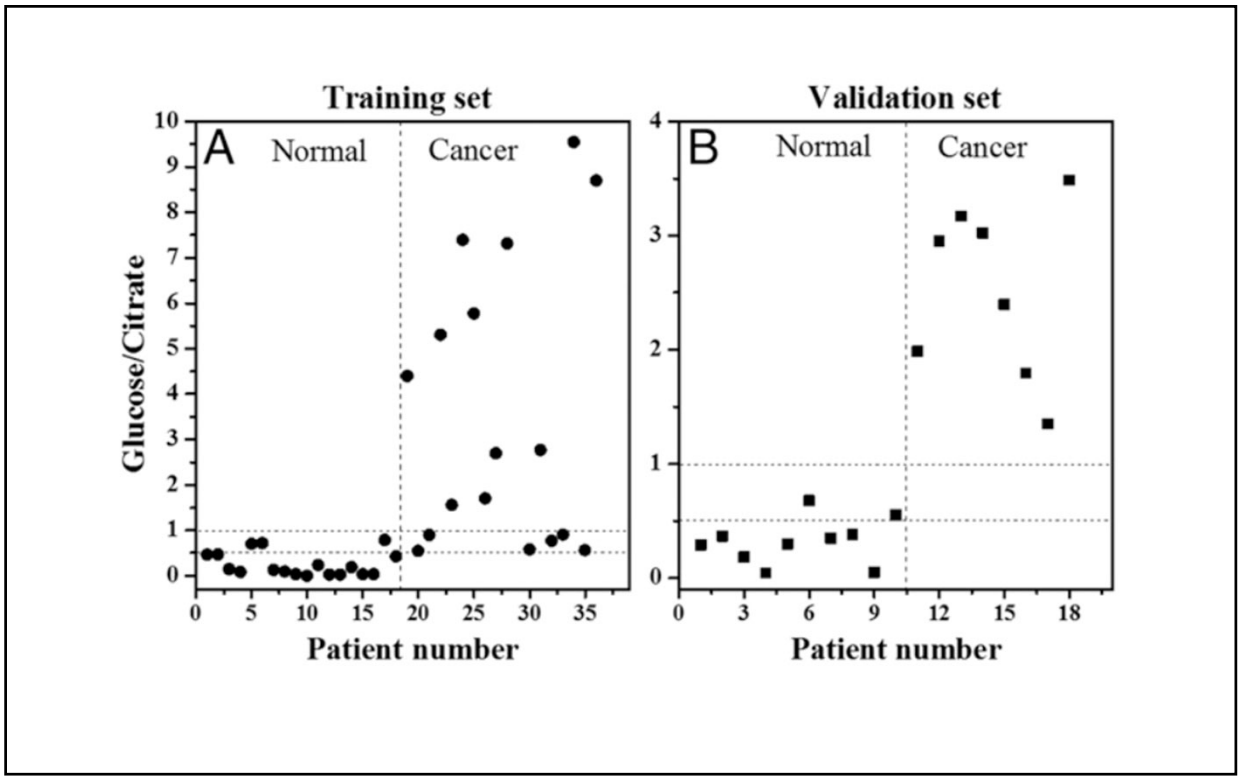
Training set
Validation set
A
B
Normal
Cancer
Glucose/Citrate
Patient number
Patient number

42

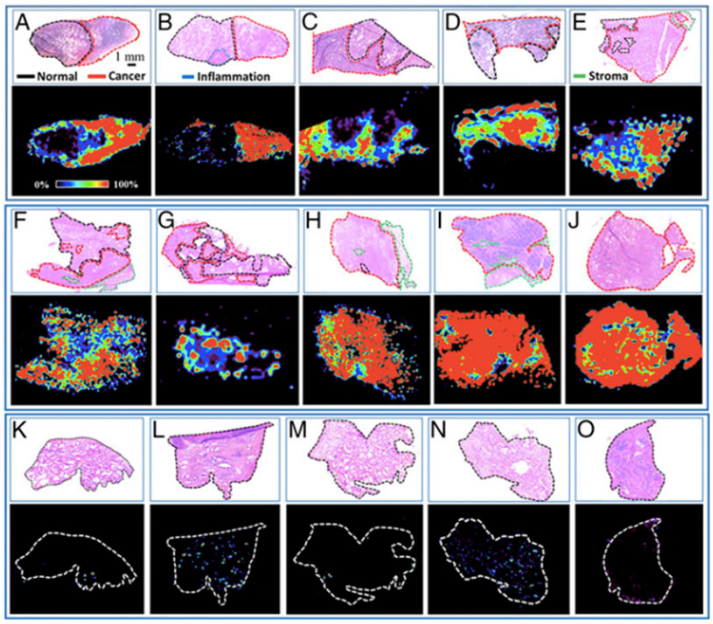

Distribution of glucose/citrate ratio of some representative prostate tissue specimens showing significant elevation of the glucose/citrate ratio in cancer. The Top of each panel (A–O) shows the histopathological evaluation (H&E) of the corresponding tissue, where cancer areas have been demarcated by **red**, benign areas by **black**, stroma areas by **green**, and inflammation areas by **blue**.

43

Use of Raman spectroscopy

Real-time imaging of metabolites in skin

- http://harvard.sunneyxielab.org/research/carstechniques.htm

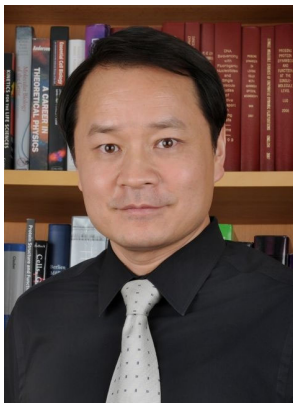

Sunny Xie, PhD – ex-Harvard, now in Beijing

https://www.sunneyxielab.org/en_home/

44

Where to next?

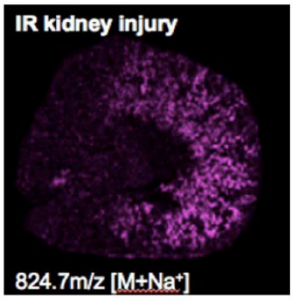

MALDI-Imaging of a phospholipid
Janusz Kabarowski/Kelly Walters

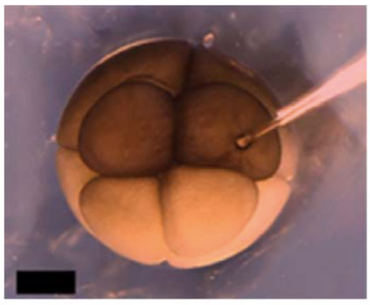

Multiple sampling single cells – Nemes group

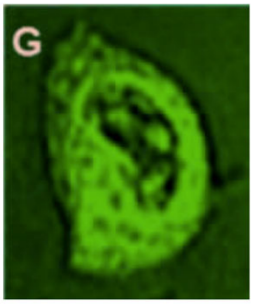

CARS imaging of a cancer cell – spectroscopic, real time Raman imaging

OR, two people with disparate abilities and insights will create something we've never heard of (yet)

45

What might it be?

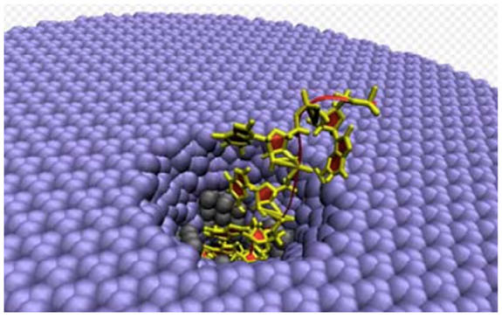

Nanoprobe inserted into the wall of a cell recording changes in metabolism in real time – sub nl sampling/analysis

TOMORROW?

Measuring O_2 uptake using a Warburg apparatus – 10 ml incubations

YESTERDAY

The O_2 and pH probes of a Seahorse™ apparatus – 7 µl incubations

TODAY

46

Publications

- Santagata S, Eberlin LS, Norton I, Calligaris D, Feldman DR, Ide JL, Liu X, Wiley JS, Vestal ML, Ramkissoon SH, Orringer DA, Gill KK, Dunn IF, Dias-Santagata D, Ligon KL, Jolesz FA, Golby AJ, Cooks RG, Agar NY. Intraoperative mass spectrometry mapping of an onco-metabolite to guide brain tumor surgery. PNAS 2014;111(30):11121-6.
- Golf O, Strittmatter N, Karancsi T, Pringle SD, Speller AV, Mroz A, Kinross JM, Abbassi-Ghadi N, Jones EA, Takats Z. Rapid evaporative ionization mass spectrometry imaging platform for direct mapping from bulk tissue and bacterial growth media. Anal Chem. 2015 Mar 3;87(5):2527-34.
- Balog J, Kumar S, Alexander J, Golf O, Huang J, Wiggins T, Abbassi-Ghadi N, Enyedi A, Kacska S, Kinross J, Hanna GB, Nicholson JK, Takats Z. In vivo endoscopic tissue identification by rapid evaporative ionization mass spectrometry (REIMS). Angew Chem Int Ed Engl. 2015 Sep 14;54(38):11059-62.
- Banerjee S, Zarea RN, Tibshirani RJ, Kunder CA, Nolley R, Fan R, Brooks JD, Sonn GA. Diagnosis of prostate cancer by desorption electrospray ionization mass spectrometric imaging of small metabolites and lipids. PNAS early edition, March 2017
- St John ER, Balog J, McKenzie JS, Rossi M, Covington A, Muirhead L, Bodai Z, Rosini F, Speller AVM, Shousha S, Ramakrishnan R, Darzi A, Takats Z, Leff DR. Rapid evaporative ionisation mass spectrometry of electrosurgical vapours for the identification of breast pathology: towards an intelligent knife for breast cancer surgery. Breast Cancer Res. 2017 May 23;19(1):59.
- Phelps DL, Balog J, Gildea LF, Bodai Z, Savage A, El-Bahrawy MA, Speller AV, Rosini F, Kudo H, McKenzie JS, Brown R, Takáts Z, Ghaem-Maghami S. The surgical intelligent knife distinguishes normal, borderline and malignant gynaecological tissues using rapid evaporative ionisation mass spectrometry (REIMS). Br J Cancer. 2018 May;118(10):1349-1358.

47

More publications

- Alfaro CM, Pirro V, Keating MF, Hattab EM, Cooks RG, Cohen-Gadol AA. Intraoperative assessment of isocitrate dehydrogenase mutation status in human gliomas using desorption electrospray ionization-mass spectrometry. J Neurosurg. 2019 Jan 4;132(1):180-187.
- Pu F, Alfaro CM, Pirro V, Xie Z, Ouyang Z, Cooks RG. Rapid determination of isocitrate dehydrogenase mutation status of human gliomas by extraction nanoelectrospray using a miniature mass spectrometer. Anal Bioanal Chem. 2019 Feb 2. doi: 10.1007/s00216-019-01632-5.
- Hänel L, Kwiatkowski M, Heikaus L, Schlüter H. Mass spectrometry-based intraoperative tumor diagnostics. Future Sci OA. 2019 Mar 7;5(3):FSO373.
- Tzafetas M, Mitra A, Paraskevaidi M, Bodai Z, Kalliala I, Bowden S, Lathouras K, Rosini F, Szasz M, Savage A, Balog J, McKenzie J, Lyons D, Bennett P, MacIntyre D, Ghaem-Maghami S, Takats Z, Kyrgiou M. The intelligent knife (iKnife) and its intraoperative diagnostic advantage for the treatment of cervical disease. Proc Natl Acad Sci U S A. 2020 Mar 16.
- Kuzmin AN, Pliss A, Rzhevskii A, Lita A, Larion M. *BCAbox* Algorithm Expands Capabilities of Raman Microscope for Single Organelles Assessment. Biosensors (Basel). 2018 Nov 10;8(4):106
- Ruiz-Rodado V, Lita A, Larion M. Advances in measuring cancer cell metabolism with subcellular resolution. Nat Methods. 2022 Sep;19(9):1048-1063.

48